Predicted Performance of Semiconductor Junction Circulators with Losses

Lionel E. Davis, *Senior Member, IEEE,* and Robin Sloan, *Member, IEEE*

***Abstract*—A study of the circulation properties of a gyroelectric medium consisting of a high-quality n-type semiconductor is given. Losses due to electron collisions are modeled by inclusion of the collision frequency ν_c in the relative permittivity tensor. Broadband low-loss operation of a semiconductor slotline junction circulator above the extraordinary wave resonance frequency f_{res} appears possible at near-millimetric frequencies. Larger, applied static magnetic fields enable narrowband low-loss operation at frequencies below the resonance at f_{res}.**

A 40 GHz design is described for GaAs cooled to 77 K. The minimum inband insertion loss is 0.82 dB. InSb theoretically possesses still lower losses for a reduced applied magnetic field. An example at an operating frequency of 75 GHz in InSb is given.

I. Introduction

ANALYSIS of the ferrite junction circulator is well understood [1], [2]. Such ferrite designs provide broadband impedance tracking performance up to 40 GHz. Above this frequency ferrite designs are limited to narrowband operation, since the maximum saturation magnetization available is about 5500 G. In this paper low-loss semiconductor slotline junction circulators [3] are predicted by applying the Green's function approach to the Drude–Zener model of semiconductors, and these components could be used in microstrip circuits by incorporating the usual transitions [4]. The performance of an ideal (lossless) semiconductor junction circulator was discussed earlier [5] by extending the gyromagnetic analysis [1] to the gyroelectric case, which employs magnetoplasmons. In this paper microwave losses due to electron collisions are examined in the context of device performance. In the study presented here, high-quality n-type gallium arsenide and indium antimonide cooled to 77 K are considered. Losses in the semiconductors are modeled by incorporating the electron collision frequency ν_c, into the relative permittivity tensor. In GaAs, ν_c is taken to be 1.3×10^{11}/s (corresponding to a mobility of 2×10^5 cm^2/V · s) [6], and in InSb ν_c is calculated to be 1.5×10^{11}/s (corresponding to a mobility of 8.3×10^5 cm^2/V · s) [7]–[9].

Manuscript received March 31, 1993; revised June 15, 1993. This work was supported in part by the University of Manchester Institute of Science and Technology (UMIST), and by the Defense Research Agency, U.K.

The authors are with the Department of Electrical Engineering, University of Manchester Institute of Science and Technology, Manchester, United Kingdom M60 1QD.

IEEE Log Number 9213019.

The maximum easily available magnetic field strength is estimated to be 4000 G, which yields a cyclotron frequency of $\omega_c = 1.05 \times 10^{12}$ rad/s in GaAs. Such a semiconductor magnetized uniformly in the z-direction possesses the tensor relative permittivity in cylindrical coordinates given by (1) [6].

$$[\epsilon] = \begin{bmatrix} \epsilon & -j\kappa & 0 \\ +j\kappa & \epsilon & 0 \\ 0 & 0 & \zeta \end{bmatrix} \tag{1}$$

where

$$\epsilon = \epsilon_r - \frac{\omega_p^2(\omega - j\nu_c)}{\omega\left[(\omega - j\nu_c)^2 - \omega_c^2\right]} \tag{2}$$

$$\kappa = \frac{\omega_p^2\omega_c}{\omega\left[(\omega - j\nu_c)^2 - \omega_c^2\right]} \tag{3}$$

$$\zeta = \epsilon_r - \frac{\omega_p^2}{\omega(\omega - j\nu_c)} \tag{4}$$

and ω_p is the plasma frequency defined by $\omega_p = \sqrt{(Ne^2/m^*\epsilon_o)}$ rad/s and $\omega_c = |e|B_o/m^*$ rad/s. Here, N is the density of "nearly free" electrons in the semiconductor, m^* is the effective electron mass, and ϵ_r is the static dielectric constant. All other symbols have their usual meanings.

II. Semiconductor Disk

The boundary conditions for a semiconductor slotline disk circulator are the dual of those found in the analogous ferrite stripline circulator. An electric wall is present at a radius $r = R$ except at each port where the electromagnetic fields are assumed uniform over the angle subtended by each connecting slotline 2ψ. This is illustrated in Fig. 1 and by (5). On the top and bottom of the disk there are magnetic walls.

$$E_\phi(R, \phi) = \begin{cases} A & -\dfrac{\pi}{3} - \psi < \phi < -\dfrac{\pi}{3} + \psi \\ B & \dfrac{\pi}{3} - \psi < \phi < \dfrac{\pi}{3} + \psi \\ C & \pi - \psi < \phi < \pi + \psi \\ 0 & \text{elsewhere.} \end{cases} \tag{5}$$

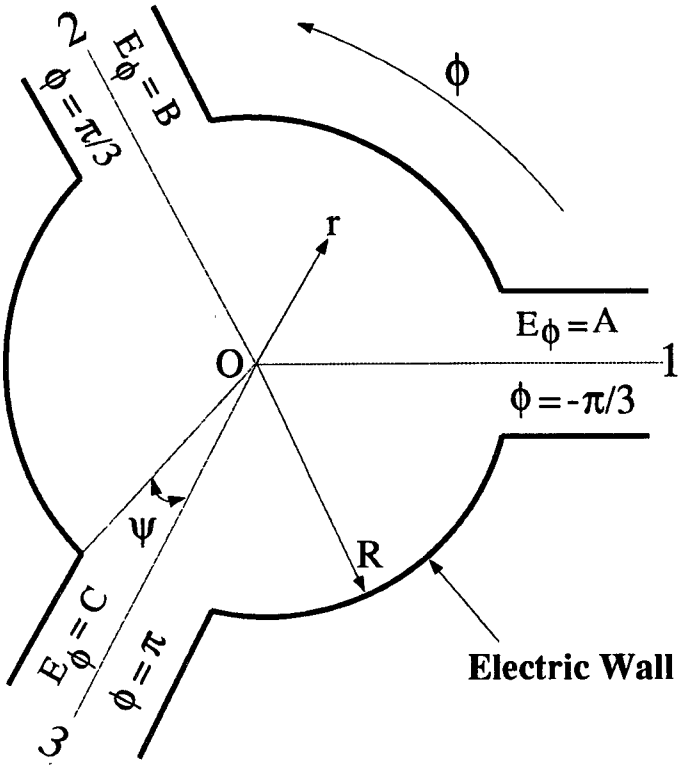

Fig. 1. Boundary conditions on the semiconductor disk with slotline feeds.

The semiconductor disk is considered to be sufficiently thin as to prevent field variation in the disk in the z-direction. The problem is then reduced to two of three dimensions. The relative permittivity tensor of (1) is then applied to Maxwell's equations to produce (6) and (7).

$$E_\phi = -\frac{1}{j\omega\epsilon_o\epsilon_{eff}}\left\{j\frac{\kappa}{\epsilon}\cdot\frac{1}{r}\frac{\partial H_z}{\partial\phi} + \frac{\partial H_z}{\partial r}\right\} \tag{6}$$

$$E_r = \frac{1}{j\omega\epsilon_o\epsilon_{eff}}\left\{\frac{1}{r}\frac{\partial H_z}{\partial\phi} - j\frac{\kappa}{\epsilon}\frac{\partial H_z}{\partial r}\right\} \tag{7}$$

where

$$\epsilon_{\text{eff}} = \frac{\epsilon^2 - \kappa^2}{\epsilon}. \tag{8}$$

The Helmholtz equation in H_z for the TE_{nm} modes is given in (9):

$$\frac{\partial^2 H_z}{\partial r^2} + \frac{1}{r}\frac{\partial H_z}{\partial r} + \frac{1}{r^2}\frac{\partial^2 H_z}{\partial\phi^2} + k^2 H_z = 0 \tag{9}$$

where

$$k^2 = \omega^2\mu_o\epsilon_o\epsilon_{\text{eff}}. \tag{10}$$

The general solution to this equation for $\epsilon_{\text{eff}} \geq 0$ and realizable finite magnetic field at zero radius is given by

$$H_{z,n}(r, \phi) = a_n J_n(kr)e^{jn\phi} \tag{11}$$

where a_n are constants, and J_n is the nth order Bessel function of the first kind.

If the effective permittivity is negative, then the solution to the Helmholtz equation requires modified Bessel functions. The lossy terms in the tensor permittivity make the effective permittivity of (8) complex and hence the Bessel functions in the general solution also become complex.

As with ferrites, the ratio of the lossless ($\nu_c = 0$) tensor terms κ/ϵ, and the effective relative permittivity ϵ_{eff} are important parameters and are plotted in Figs. 2 and 3. Typical values of the cyclotron frequency, plasma frequency, and static dielectric constant are taken for uniformly magnetized GaAs at 77 K [6]. The response of κ/ϵ is similar to the ratio κ/μ experienced with ferrites, but is nonzero at very low frequencies. Also, for ferrites the equivalent variable expression to ϵ_{eff}, that is, $\mu_{\text{eff}} = \mu^2 - \kappa^2/\mu$ is zero at only one frequency.

In Figs. 2 and 3 asymptotic behavior occurs at f_{res} where

$$\omega_{\text{res}} = 2\pi f_{\text{res}} = \sqrt{\omega_c^2 + \frac{\omega_p^2}{\epsilon_r}} \tag{12}$$

and this is referred to as the extraordinary wave resonance angular frequency. The angular frequencies at which the magnitude of κ/ϵ is unity are ω_A, ω_c, and ω_B, where,

$$\omega_A = 2\pi f_A = \frac{\omega_c}{2}\left[\sqrt{1 + \frac{4\omega_p^2}{\epsilon_r\omega_c^2}} - 1\right] \tag{13}$$

$$\omega_B = 2\pi f_B = \frac{\omega_c}{2}\left[\sqrt{1 + \frac{4\omega_p^2}{\epsilon_r\omega_c^2}} + 1\right]. \tag{14}$$

Also, notice ω_A and ω_B are separated in frequency by ω_c and at ω_A and ω_B, $\epsilon_{\text{eff}} = 0$.

In ferrite circulators values of the gyromagnetic ratio $|\kappa/\mu|$ between zero and unity are generally used. In this gyroelectric solution there are two regions where the magnitude of κ/ϵ is less than unity. One above and one below the extraordinary wave resonance frequency. Inspection of (2) and (3) reveals that if the imaginary parts of ϵ and κ are to be small either $\omega_c >> \nu_c$ or $\omega >> \nu_c$. Also note from the denominators of (2) and (3) that the signal frequency ω should not be in close proximity to ω_c, otherwise there will be a cancellation of the real terms, and the collision frequency will become the dominating term.

The boundary conditions (5) determine the electric field E_ϕ at the disk edge. H_z is determined by following Bosma's analysis [1] as in [5]; to produce a Green's function that describes the field intensities anywhere on the disk. The Green's function employed here at a radius $r = R$ is given in (15).

$$G(\phi, \phi') = -\frac{jJ_o(x)}{2\pi Z_{\text{eff}}J_o'(x)} + \frac{1}{\pi Z_{\text{eff}}}\sum_{n=1}^{\infty}\frac{\frac{\kappa}{\epsilon}\cdot\frac{n}{x}J_n^2(x)\sin[n\theta] - jJ_n'(x)J_n(x)\cos[n\theta]}{\{J_n'(x)\}^2 - \left\{\frac{\kappa}{\epsilon}\frac{n}{x}J_n(x)\right\}^2} \tag{15}$$

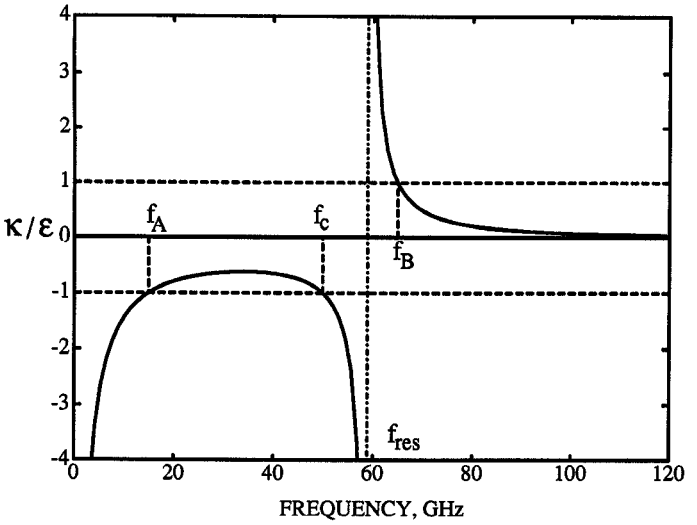

Fig. 2. Ratio of tensor entries κ/ϵ versus frequency: (f_c = 50 GHz, f_p = 107.8 GHz, ϵ_r = 12.0, and ν_c = 0).

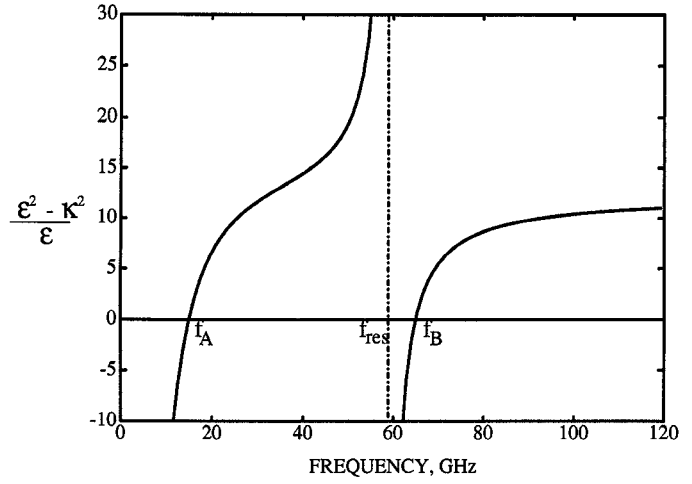

Fig. 3. Variation of effective permittivity ϵ_{eff} with frequency: (f_c = 50 GHz, f_p = 107.8 GHz, ϵ_r = 12.0, and ν_c = 0).

where $x = kR$, $\theta = \phi - \phi'$, and the extraordinary wave impedance of the unbounded plasma is

$$Z_{\text{eff}} = \sqrt{\frac{\mu_o}{\epsilon_o \epsilon_{\text{eff}}}}. \tag{16}$$

The integrated Green's function is defined as

$$\overline{G}(\phi;\, \phi') = \frac{1}{2\psi} \int_{\phi-\psi}^{\phi+\psi} \int_{\phi'-\psi}^{\phi'+\psi} G(\phi;\, \phi')\, d\phi'\, d\phi. \tag{17}$$

Substituting (15) into (17) gives (18).

III. Scattering Parameters of Lossless Designs

The scattering parameters for the gyroelectric case can be determined as described in [5]. For the lossless cyclic symmetrical three-port the scattering matrix can be written as

$$[S] = \begin{bmatrix} \alpha & \gamma & \beta \\ \beta & \alpha & \gamma \\ \gamma & \beta & \alpha \end{bmatrix} \tag{19}$$

where the scattering parameters are given in (20)–(22):

$$\alpha = -1 - \frac{j\pi Z_{\text{eff}} Y_d [Q_1^2 - Q_2 Q_3]}{[Q_1^3 + Q_2^3 + Q_3^3 - 3Q_1 Q_2 Q_3]} \tag{20}$$

$$\beta = -\frac{j\pi Z_{\text{eff}} Y_d [Q_2^2 - Q_1 Q_3]}{[Q_1^3 + Q_2^3 + Q_3^3 - 3Q_1 Q_2 Q_3]} \tag{21}$$

$$\gamma = -\frac{j\pi Z_{\text{eff}} Y_d [Q_3^2 - Q_1 Q_2]}{[Q_1^3 + Q_2^3 + Q_3^3 - 3Q_1 Q_2 Q_3]} \tag{22}$$

and Y_d is the intrinsic admittance of the dielectric in the slotline at each port, i.e.,

$$Y_d = \frac{1}{Z_d} = \sqrt{\frac{\epsilon_o \epsilon_d}{\mu_o}} \tag{23}$$

and Q_1, Q_2, and Q_3 are defined as

$$Q_1 = \frac{j\pi Z_{\text{eff}}}{2} \left[\overline{G}\left(-\frac{\pi}{3};\, -\frac{\pi}{3}\right) - Y_d \right] \tag{24}$$

$$Q_2 = \frac{j\pi Z_{\text{eff}}}{2} \overline{G}\left(-\frac{\pi}{3};\, \frac{\pi}{3}\right) \tag{25}$$

$$Q_3 = \frac{j\pi Z_{\text{eff}}}{2} \overline{G}\left(-\frac{\pi}{3};\, \pi\right). \tag{26}$$

The lossless circulation equations can then be derived by assuming that for perfect circulation either the scattering matrix element β is zero or γ is zero. The principal solutions to the circulation equations are shown in Fig. 4(a) and (b).

Wu and Rosenbaum [2] produced similar curves for the ferrite disk for varying κ/μ. Those presented here differ in the respect that in Fig. 4(b); Z_d/Z_{eff} is plotted rather than the inverse.

$$\overline{G}(\phi,\, \phi') = -\frac{jJ_o(x)\psi}{\pi Z_{\text{eff}} J_o'(x)} + \frac{2}{\pi Z_{\text{eff}}} \sum_{n=1}^{\infty} \frac{\sin^2(n\psi)}{n^2\psi} \frac{\frac{\kappa}{\epsilon} \cdot \frac{n}{x} J_n^2(x) \sin[n\theta] - jJ_n'(x)\, J_n(x) \cos[n\theta]}{\{J_n'(x)\}^2 - \left\{\frac{\kappa}{\epsilon} \frac{n}{x} J_n(x)\right\}^2} \tag{18}$$

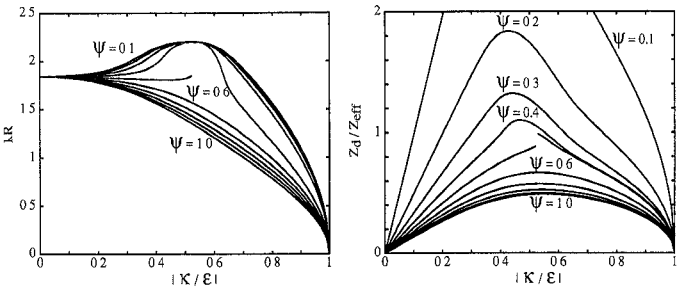

Fig. 4. (a) Solution of the first circulation equation. (b) Solution of the second circulation equation.

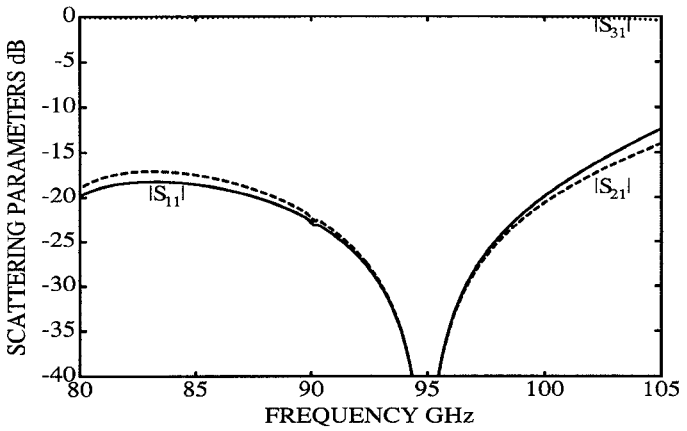

Fig. 5. Predicted performance of idealized GaAs circulator at 77 K, R = 0.361 mm, ψ = 0.7 rad.

IV. Circulation Above the Extraordinary Wave Resonance Frequency

In the lossless case the effective permittivity is negative between the extraordinary wave resonance frequency and the radial frequency ω_B, as illustrated in Fig. 3. As stated earlier, this requires solutions in terms of modified Bessel functions in the Green's function of (15) and (17). Ideal circulation in this region is not shown in Fig. 4, since the ratio of κ/ϵ will be greater than unity. The broadband design given earlier [5] and illustrated in Fig. 5 operates in this region, and above the frequency f_B, where κ/ϵ is less than unity. The 25 dB isolation bandwidth is 6.9 percent. A plasma frequency was chosen for the idealized, n-type GaAs to be $f_p/\sqrt{\epsilon_r}$ = 60.0 GHz and a cyclotron frequency of f_c = 50.0 GHz. The variation in κ/ϵ is from unity at 90 GHz to 0.52 at 98 GHz. The function of Z_d/Z_{eff} versus κ/ϵ can be calculated over the frequency range of interest, assuming an dielectric constant of ϵ_d = 10.0 at the three ports. Comparing the calculated curves in Z_d/Z_{eff} with those produced by the second circulation condition [Fig. 4(b)] enables a half-angle ψ to be selected. Then the radius can be determined from the first circulation condition [Fig. 4(a)]. This is based on the Wu and Rosenbaum method except that the curves for Z_d/Z_{eff} must be calculated for each frequency point.

In this example, the half-angle was found to be 0.7 rad and the radius 0.361 mm. This design method does not however consider the losses due to electron collisions. For GaAs at 77 K the momentum relaxation time $\tau = 8 \times 10^{-12}$ [6], and $\omega_c\tau > 1$, which is a prerequisite for effective interaction between the carriers and the electromagnetic fields. Furthermore, by inspection of (2) and (3) it can be seen that the losses become less significant with increasing, static magnetic field. Therefore, if a relatively large cyclotron frequency is necessary for a low insertion loss, then a frequency of operation above the extraordinary wave resonance frequency would imply that such designs are suitable for near-millimeter wavelengths.

V. Circulation Below the Extraordinary Wave Resonance Frequency, with Losses

At operating frequencies below ω_{res}, there is a useful range of frequencies between ω_A and ω_c where, the magnitude of the ratio of κ to ϵ is less than unity. This can be seen in Fig. 2. Notice here κ/ϵ is negative, this indicates circulation in the opposite direction to semiconductor devices operating above the extraordinary wave resonance frequency. A large cyclotron frequency enables design frequencies in this region to extend up to millimetric wavelengths. This can be generated by either a large, static magnetic field or by a combination of a moderate, static magnetic field and a low effective electron mass.

A narrowband design at 40 GHz in lossy n-type GaAs has an applied magnetic field strength of 4000 G, which produces a cyclotron angular frequency of $\omega_c = 1.05 \times 10^{12}$ rad/s. If the doping is sufficient to provide a plasma frequency (f_p), of 100 GHz at 77 K, then the circulation conditions are fulfilled at a frequency given by an intercept at 40 GHz of a second circulation condition [Fig. 4(b)]. At this frequency the gyroelectric ratio is 0.121 and the impedance ratio Z_d/Z_{eff} = 1.105. This in turn corresponds to a half-angle ψ of 0.12 rad and a radius of 0.636 mm. The design approach here is to initially consider the plasma to be lossless and then incorporate the collision frequency into the expressions for the scattering parameters in order to calculate losses. When this is performed then the minimum insertion loss is 0.82 dB at 40 GHz, and the 20 dB isolation bandwidth is 3.7 percent. The calculated s-parameters are shown in Fig. 6. The maximum, predicted inband insertion loss is 1.0 dB and occurs at the band edges.

If instead of GaAs, the semiconductor medium is InSb cooled to 77 K using data from Sze [7] and Landbolt-Bornstein [9], the same applied magnetic field of B_o = 4000 G yields a cyclotron frequency of almost 800 GHz. If the plasma frequency is taken be the same as for the GaAs circulator (100 GHz) then the half-angle required for circulation at a signal frequency of 75 GHz is much less than 0.1 rad and as such is impracticable. Increasing the plasma frequency to 500 GHz yields a better solution for the half-angle of 0.21 rad, and disk radius of 0.31 mm. The calculated frequency performance is illustrated in Fig. 7.

The minimum theoretical insertion loss is 0.26 dB and occurs at 75 GHz, the 20 dB isolation bandwidth is 7.7 percent and the worst inband insertion loss is 0.4 dB. This design however, does not model the motion of the holes

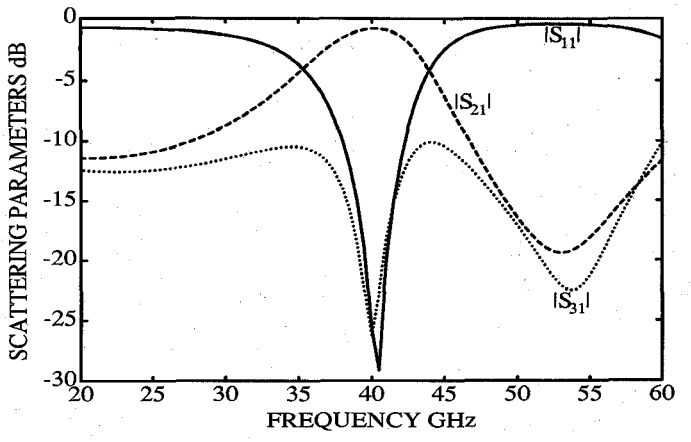

Fig. 6. Predicted performance of lossy GaAs circulator at 77 K, $R = 0.63$ mm, $\psi = 0.12$ rad, and $\nu_c = 1.3 \times 10^{11}$/s.

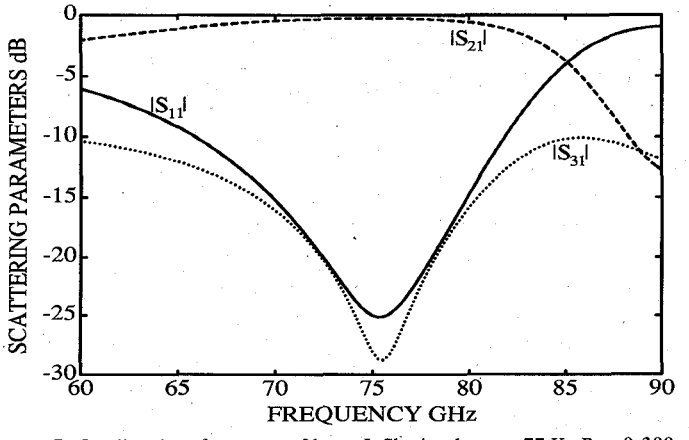

Fig. 7. Predicted performance of lossy InSb circulator at 77 K, $R = 0.309$ mm, $\psi = 0.21$ rad, and $\nu_c = 1.5 \times 10^{11}$/s.

in the semiconductor, which is relevant if $\omega_{ch}\tau_h > 1$. It has been shown by Furdyna [10] that if $\omega_{ch} << 1$ the holes have no significant effect upon the magnetoplasmons.

VI. Conclusions

The operation of a slotline junction circulator including the effect of losses due to electron collisions and assuming an operating temperature of 77 K has been described. Examples have been given of predicted performance in the frequency ranges near 40 and 75 GHz. When operating at a frequency above the extraordinary wave resonance frequency, losses become large unless the cyclotron frequency is very large. Therefore, these devices will only operate with low loss at near-millimetric frequencies, although a relatively broad bandwidth at these frequencies should be obtainable. Below the extraordinary wave resonance frequency, low-loss designs are narrowband and are based on an intercept between the normalized extraordinary wave admittance and the second circulation curve. Insertion loss is heavily dependent upon the cyclotron frequency. For a given applied magnetic field strength it initially appears that InSb is a better candidate than GaAs for low-loss circulation, having a theoretical insertion loss of only 0.26 dB at 75 GHz. Very high quality GaAs is required for high mobilities and low carrier concentrations of the order of 10^{13} cm^{-3}. Such material is not currently available, but designs may be possible using higher concentrations. The effects due to holes have not been included. These circulators may be realizable in structures such as finline and nonradiating dielectric waveguides. They may also be suitable for integration on MMIC's and in high-T_c superconducting applications.

References

[1] H. Bosma, "On stripline Y-circulation," *IEEE Trans. Microwave Theory Tech.*, pp. 61–72, Jan. 1964.
[2] Y. S. Wu and F. J. Rosenbaum, "Wide-band operation of microstrip circulators," *IEEE Trans. Microwave Theory Tech.*, vol. MTT-22, pp. 849–856, Oct. 1974.
[3] L. E. Davis, "Semiconductor junction circulators," Patent Appl. 9222553.1, Oct. 1992.
[4] K. C. Gupta, R. Garg, and I. J. Bahl, *Microstrip Lines and Slotlines*. Dedham, Mass. Artech House, 1979.
[5] L. E. Davis and R. Sloan, "Semiconductor Junction Circulators," in *IEEE Int. MTT Symp. Dig.*, vol. 1, June 1993, pp. 483–486.
[6] D. M. Bolle and S. H. Talisa, "Fundamental considerations in millimeter and near-millimeter component design employing magnetoplasmons," *IEEE Trans. Microwave Theory Tech.*, vol. MTT-29, pp. 61–72, Sept. 1981.
[7] S. M. Sze, *Physics of Semiconductor Devices*. New York: Wiley-Interscience, 1969.
[8] J. D. Wiley, P. S. Peercy, and R. N. Dexter, "Helicons and nonresonant cyclotron absorption in semiconductors. I. InSb," *Phys. Rev.*, vol. 181, pp. 1173–1181, May 1969.
[9] O. Madelung, Ed., *Landbolt-Bornstein: Numerical Data and Functional Relationships in Science and Technology*, Vol. 17, *Semiconductors of Subvolume a: Physics of Group IV Elements and III–V Compounds*. New York: Springer-Verlag, 1982.
[10] J. K. Furdyna, "Interferometer measurement of microwave helicon dispersion and the hole damping effect in intrinsic InSb," *Phys. Rev. Lett.*, vol. 14, pp. 635–638, 1965.

Lionel E. Davis (SM'65) received the B.Sc. and Ph.D. degrees from the University of Nottingham and the University of London in 1956 and 1960, respectively.

From 1959 to 1964 he was with Mullard Research Laboratories, Redhill, England, and from 1964 to 1972 he was an Assistant Professor and then Associate Professor of Electrical Engineering at Rice University, Houston, TX. From 1972 to 1987 he was with Paisley College, Scotland, where he was Professor and Head of the Department of Electrical and Electronic Engineering and, for two periods, Dean of Engineering. In 1987 he joined UMIST, where he is Professor of Communication Engineering and Head of the Department of Electrical Engineering and Electronics. His current research interests are in nonreciprocal components, gyrotropic media, high-*Tc* superconductors, and novel dielectric materials.

Dr. Davis is a Fellow of the Institution of Electrical Engineers and of the Institute of Physics. He has served on the Council and other committees of the Institution of Electrical Engineers, and on several subcommittees of the Science and Engineering Research Council. He has been a Visiting Professor at University of College London (1970–1971) and the University of California at San Diego (1978–1979) and a Consultant for Bendix Research Laboratories (1966–1968). He was a founding member of the Houston Chapter of the Microwave Theory and Techniques Society.

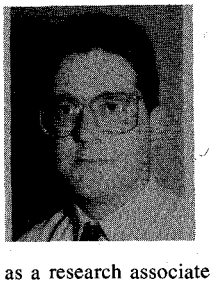

Robin Sloan (M'93) received the B.Sc. degree in electronic engineering from Sussex University, England in 1985. From 1985 to 1987 he was at British Aerospace Air Weapons Division, Hatfield, England. He then received the M.Sc. degree in communication engineering and digital electronics and the Ph.D. degree from the University of Manchester Institute of Science and Technology (UMIST) in 1988 and 1991, respectively.

From 1991 until 1992 he worked on power dividers and combiners. He is currently employed as a research associate at UMIST. His research interests include devices using gyrotropic materials, and microwave and millimeter circuits.